Global phase diagram and six-state clock universality behavior in the triangular antiferromagnetic Ising model with anisotropic next-nearest-neighbor coupling: Level-spectroscopy approach

Hiromi Otsuka and Yutaka Okabe
Department of Physics, Tokyo Metropolitan University, Tokyo 192-0397, Japan

Kiyohide Nomura
Department of Physics, Kyushu University, Fukuoka 812-8581, Japan

(Received 7 April 2006; published 11 July 2006)

We investigate the triangular-lattice antiferromagnetic Ising model with a spatially anisotropic next-nearest-neighbor ferromagnetic coupling, which was first discussed by Kitatani and Oguchi. By employing the effective geometric factor, we analyze the scaling dimensions of the operators around the Berezinskii-Kosterlitz-Thouless (BKT) transition lines, and determine the global phase diagram. Our numerical data exhibit that two types of BKT-transition lines separate the intermediate critical region from the ordered and disordered phases, and they do not merge into a single curve in the antiferromagnetic region. We also estimate the central charge and perform some consistency checks among scaling dimensions in order to provide the evidence of the six-state clock universality. Further, we provide an analysis of the shapes of boundaries based on the crossover argument.

DOI: 10.1103/PhysRevE.74.011104 PACS number(s): 64.60.−i, 05.50.+q, 05.70.Jk

I. INTRODUCTION

The antiferromagnetic Ising model on the triangular lattice may be the simplest example to possess the frustration effects. As its manifestation, the system does not complete the long-range order even in the ground state, but has the critical ground-state ensemble [1–5]. This emerging criticality due to the frustration is the Gaussian type, where the Coulomb-gas picture [6] well describes properties of elementary excitations and also singularities of physical quantities [7–9]. Meanwhile, continuum field theories for systems nearby the criticality have been well developed on the basis of the conformal symmetry; it offers, beyond the Coulomb-gas description, the unified and pervasive approaches to investigate the one-dimensional (1D) quantum and two-dimensional (2D) classical systems. Further, since they also offer us powerful strategies to numerically investigate the systems around the Gaussian fixed point, quantitative reliability becomes higher than ever before, which contributes to clarify long-standing problems in related research fields [10–13].

In this paper, we treat the triangular antiferromagnetic Ising model (TAFIM) with anisotropic next-nearest-neighbor (NNN) ferromagnetic (F) coupling [14], which we call the Kitatani-Oguchi model hereafter. The reduced Hamiltonian including temperature $\mathcal{H}=\beta H$ is given by

$$\mathcal{H}(K_1,K_2) = K_1 \sum_{\langle j,k\rangle} \delta_{\sigma_j,\sigma_k} - K_2 \sum_{[j,k]'} \delta_{\sigma_j,\sigma_k}. \qquad (1)$$

The binary variable $\sigma_j=0,1$ is on the jth site of the triangular lattice Λ which consists of interpenetrating three sublattices Λ_l $(l=0,1,2)$. The first sum runs over all nearest-neighbor (NN) pairs $\langle j,k\rangle$, whereas the second over NNN pairs $[j,k]'$ *in two of the three directions* (see Fig. 1). Although the model was introduced due to a technical reason in their numerical calculation, unlike in the isotropic NNN F coupling case, it provides an opportunity to investigate an important effect, i.e., the spatial anisotropy in critical phenomena.

Since its introduction, there is a belief that the model (1) is not strongly anisotropic and belongs to the six-state clock (6SC) universality class as the isotropic model does (for more severe anisotropies, see [12,15]). Thus, two types of Berezinskii-Kosterlitz-Thouless (BKT) transition lines are expected to separate the critical region from the ordered and disordered phases [18,19]. Actually, Kitatani and Oguchi (KO) performed the transfer-matrix (TM) calculations at the ratio $K_2/K_1=0.5$ in order to evaluate the β function within the Roomany-Wyld approximation [20] and the spin-spin correlation function, and then concluded the existence of the critical finite temperature region [14]. Subsequently, Miyashita, Kitatani, and Kanada performed large scale Monte Carlo (MC) simulation calculations and found the consistent results [21]. Using the cluster TM method (an approximation), Pajerský and Šurda stated that the intermediate phase possessed an incommensurate nature [22]. Contrary to these, de Queiroz and Domany performed the TM calculations, and

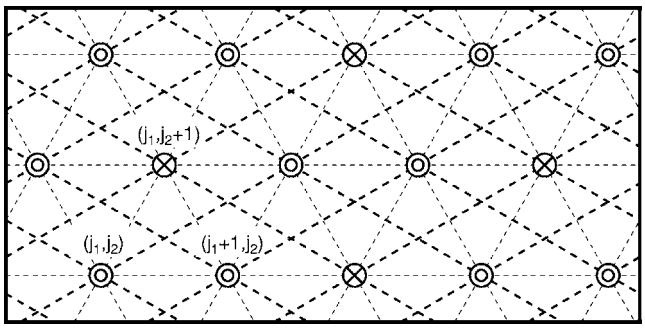

FIG. 1. The schematic representation of Hamiltonian (1). The jth site is specified by two integers (j_1,j_2) as labeled in the figure. The dotted (dashed) lines show the NN AF (anisotropic NNN F) coupling. An example of the spin configurations with the $\sqrt{3}\times\sqrt{3}$ structure is exhibited, where the spins on two (one) of three sublattices $\Lambda_{0,1}$ (Λ_2) are up ⊙ (down ⊗).

reported limited evidence for an existence of the BKT phase on the basis of the phenomenological renormalization-group (PRG) analysis [23]. They argued that this limitation was due to the lack of sixfold symmetry, and they also provided the qualitative phase diagram with a multicritical point. Quite recently, Qian and Blöte succeeded in obtaining the phase diagram of TAFIM with isotropic NNN F coupling using both TM and MC calculations, whereas, for present model, they stated that an application of the conformal mapping became difficult [24]. Considering all these together, there still exist some unclear points due to the nature of the BKT transitions and/or the effects of the anisotropy.

In this paper, we shall provide the global phase diagram of the Kitatani-Oguchi model (1) on the basis of the TM calculation data. Note especially, our result exhibits that the phase diagram possesses the same structure as that of the isotropic model [7,24]. Therefore, this provides evidence to support KO's motivation and confirms the present model being in the 6SC universality class, independently of the spatial anisotropy.

The organization of this paper is as follows: In Sec. II, we shall discuss the effective field theory to describe the low-energy and long-distance behaviors of the model, where the effects of the NN and the anisotropic NNN couplings are explained. Simultaneously, since we shall employ the level-spectroscopy method to treat the two types of BKT transitions [25], we address some relevant issues necessary for its application. In Sec. III, we shall give our numerical estimates of the phase boundary lines. By introducing the parameter-dependent geometric factor to obtain the isotropic description of the model in the 2D Euclidean space and by evaluating the factor on the basis of the conformal field theory (CFT), we check the criticality of the system and some universal relations among the scaling dimensions. The last section, Sec. IV, is devoted to the discussion and the summary of our research. We provide the analysis of the shapes of boundaries based on the crossover argument. We also compare our data with previous research results, and then give some comments.

II. THEORETICAL DESCRIPTION AND NUMERICAL CALCULATION METHOD

A. Effective field theory in the sine-Gordon language

We shall start by referring to relating results in the literature. In the exactly solved case $K_2=0$, the system shows the 2D Gaussian criticality at $K_1=\infty$. In the scaling limit of the lattice spacing $a\to 0$, but keeping $\mathbf{x}=(x_1,x_2)=(aj_1,aj_2/\zeta)$ finite [$\zeta=2/\sqrt{3}$ is the geometric factor for the triangular lattice], its effective description is given by the Lagrangian density

$$\mathcal{L}_0[\phi]=\frac{1}{2\pi K}[\nabla\phi(\mathbf{x})]^2, \tag{2}$$

where K $(=\frac{1}{2})$ is the Gaussian coupling and the phase field satisfies the periodicity condition $\sqrt{2}\phi+2\pi=\sqrt{2}\phi$ [7,9]. Reflecting the discreteness of height variables h_j in the triangular Ising solid-on-solid model which is obtained fromthe zero-temperature TAFIM [5], there exists the nonlinear potential $\cos 6\sqrt{2}\phi$. However, it is highly irrelevant at the point [7,9], so here we dropped it (see below). Writing $s_j=e^{i\pi\sigma_j}$ and the distance between jth and kth sites $r_{jk}=|\mathbf{x}-\mathbf{x}'|$, then the asymptotic behavior of the spin-spin correlation function is given as $\langle s_j s_k\rangle \simeq A\cos\varphi_{jk}/r_{jk}^{1/2}+B/r_{jk}^{9/2}$, where $\varphi_{jk}=\varphi_j-\varphi_k$ and a sublattice dependent phase $\varphi_j:=\sum_{l=0,1,2}\sum_{i\in\Lambda_l}(2\pi l/3)\delta_{i,j}$ (A, B constants.) [4,7]. Thus, the scaling dimensions of the uniform and staggered magnetizations s and S constructed through a coarse graining of s_j and $e^{\pm i\varphi_j}s_j$ with respect to each elementary triangle are given by $x_s=\frac{9}{4}$ and $x_S=\frac{1}{4}$, respectively.

Next, we move on to the anisotropic case $K_2\neq 0$. As asserted by KO, there is a plausible reason to expect that anisotropic NNN F coupling plays the same role as the isotropic one [14], i.e., it only reduces the Gaussian coupling down to a certain value [7]. However, there is no reason to expect that $\zeta=2/\sqrt{3}$ is appropriate to obtain a rotationally invariant description of the model in the 2D Euclidean space. This is because $\zeta=2/\sqrt{3}$ can express the geometric structure of the lattice Λ, but the anisotropic coupling requires a further rescaling factor, which must be incorporated multiplicatively into the geometric factor. Therefore, we suppose that the effective value of the geometric factor ζ is not known *a priori* and depending on the coupling values. In some systems including those in somewhat different situation, the anisotropy effect has been discussed [15–17], and further it is also important in the 1D quantum systems described by the Tomonaga-Luttinger-liquid Hamiltonian [26]

$$H_{\mathrm{TLL}}(v,K)=\int dx\frac{v}{2\pi}[K(\partial_x\Theta)^2+K^{-1}(\partial_x\Phi)^2], \tag{3}$$

where $[\Phi(x),\partial_{x'}\Theta(x')/\pi]=i\delta(x-x')$, and v is the velocity of an elementary excitation. While, in the imaginary-time formalism, the $(1+1)$ space-time is treated as 2D Euclidean, $\mathbf{x}=(x,v\tau)$, so as to extract the Lagrangian density (2), v as well as K, depends on the lattice-model parameters. Returning to our case, as we will see below, this dependence indeed requires an extra procedure to estimate ζ in numerical calculations, but this changes nothing of the theoretical description, *provided* ζ *is chosen properly*. Therefore, we advance our argument.

For large enough K_2, the Gaussian criticality is lifted and the sixfold-degenerate ordered state with the $\sqrt{3}\times\sqrt{3}$ sublattice structure is stabilized (see Fig. 1). On the other hand, for small K_2, the thermal scaling field $u=e^{-K_1}$ introduces the relevant energy-density perturbation (its bosonized expression is $\epsilon=\sqrt{2}\cos\sqrt{2}\theta$ in terms of θ being dual to ϕ) and brings about the disordered state [7]. In summary, these are described by the dual sine-Gordon model whose Lagrangian density is given by

$$\mathcal{L}=\mathcal{L}_0+\frac{1}{2\pi\alpha^2}(y_\phi\cos 6\sqrt{2}\phi+y_\theta\cos\sqrt{2}\theta), \tag{4}$$

where $y_\phi<0$ (see below) and $y_\theta\propto u$ are the coupling constants [27]. α is a short-distance cutoff. Since the nonlinear terms in Eq. (4) are both irrelevant in the region $\frac{1}{4}\geq K\geq\frac{1}{9}$, the present model (1) may possess two BKT-transition lines

[19]. We define $v=e^{K_2}$ and denote the upper- and lower-temperature boundaries as $v_U(u)$ and $v_L(u)$ [note $v_U(u)<v_L(u)$] for convenience, then their precise determinations are our main goal.

Quite recently, Matsuo and Nomura investigated the classical 2D 6SC model [13]. Especially, mapping it to the 1D quantum 6SC model with the explicit duality relation, they succeeded in determining two BKT transition points, where the crossings of levels observed in the systems with periodic and twisted boundary conditions were used. Although their criteria may also be efficient to our case, an implementation of the twisted boundary condition is unclear at present. On the other hand, we have also treated the BKT transitions observed in the AF three-state Potts model with the NNN F coupling by employing rather naive criteria [11]. Therefore, we shall employ the same approach in the following (see also [12]).

B. Finite-size estimates of BKT-transition points in upper and lower temperatures

First, let the system around $v_U(u)$ be considered where $\cos 6\sqrt{2}\phi$ is irrelevant. Then, it is well described by

$$\mathcal{L}_1 \simeq \mathcal{L}_0 + \frac{y_\theta}{2\pi\alpha^2}\cos\sqrt{2}\theta \quad \left(K \simeq \frac{1}{4}\right). \tag{5}$$

With respect to the determination of the BKT-transition points, one of the authors (K.N.) pointed out the importance of marginal operators [25]: Especially, in this case, $\mathcal{M}=(1/K)(\nabla\phi)^2$ and $\epsilon=\sqrt{2}\cos\sqrt{2}\theta$ hybridize along the RG flow and result in two orthogonalized operators, i.e., the "$\mathcal{M}$-like" and the "cos-like" operators. We denote the former and latter as O_0 and O_1, and define the system on Λ with M $(\to\infty)$ rows of L (a multiple of 3) sites wrapped on a cylinder, say $\Lambda(L\times\infty)$. Then, according to the conformal perturbation theory, their renormalized scaling dimensions near the multicritical point $(y_0,y_1)=(1/2K-2,y_\theta)=(0,0)$ are given as $x_0(l)\simeq 2-y_0(1+\frac{4}{3}t)$ and $x_1(l)\simeq 2+y_0(2+\frac{4}{3}t)$, respectively, where $l=\ln L$ and a small deviation from the BKT-transition point $t=y_1/y_0-1$. On the BKT line, $y_0=y_1\simeq 1/l$. On the other hand, another important operator is the uniform magnetization, $s=\sqrt{2}\cos 3\sqrt{2}\phi$ in its bosonized form, whose dimension is $x_s(l)\simeq\frac{9}{16}(2-y_0)$ in the same region. Consequently, the level-crossing condition,

$$x_0(l) = \frac{16}{9}x_s(l), \tag{6}$$

provides a finite-size estimate of $v_U(u)$, $v_U(u,L)$.

Next, we consider a region near $v_L(u)$ where $\cos\sqrt{2}\theta$ is irrelevant. Then, the effective Lagrangian density is

$$\mathcal{L}_2 \simeq \mathcal{L}_0 + \frac{y_\phi}{2\pi\alpha^2}\cos 6\sqrt{2}\phi \quad \left(K \simeq \frac{1}{9}\right). \tag{7}$$

In this case, $\mathcal{M}$ and $\sqrt{2}\cos 6\sqrt{2}\phi$ hybridize and result in the $\mathcal{M}$-like and cos-like operators, O_2 and O_3, respectively. By redefining the coupling constants $(y_0,y_1)=(18K-2,-y_\phi)$, we obtain the scaling dimensions $x_2(l)\simeq 2-y_0(1+\frac{4}{3}t)$ and $x_3(l)\simeq 2+y_0(2+\frac{4}{3}t)$ near the transition point. Since the uniform magnetization has the dimension $x_s(l)\simeq\frac{1}{4}[2-y_0(1+2t)]$, the level-crossing condition for $v_L(u,L)$ may be given by

$$x_2(l) = 4x_s(l). \tag{8}$$

Here, let the following be observed: Since we have supposed $y_\phi<0$, the sixfold-degenerate ordered states correspond to the six locking points of the phase variable, i.e., $\langle\sqrt{2}\phi\rangle\simeq\pi q/3,(q=0,1,\ldots,5)$. According to the bosonized expressions, the averages of the uniform and staggered magnetizations $[S=\exp(\pm i\sqrt{2}\phi)]$ take values $\langle s\rangle\propto e^{i\pi q}$ and $\langle S\rangle\propto e^{\pm i\pi q/3}$ in the ordered states. These are consistent with the relationship between the phase values and the spin configurations given in Refs. [7,28].

C. Discrete symmetry properties of excitations

Now, let us consider the system on $\Lambda(L\times\infty)$, and define the transfer matrix, $\mathbf{T}(L)$, connecting the NNN rows in the vertical direction of Fig. 1. We denote its eigenvalues as $\lambda_p(L)$ or their logarithms as $E_p(L)=-\frac{1}{2}\ln|\lambda_p(L)|$ (p specifies a level). Then, the conformal invariance provides direct expressions of the central charge c, the scaling dimension x_p, and the conformal spin s_p in the critical systems as follows [29,30]:

$$E_g(L) \simeq Lf - \frac{\pi}{6L\zeta}c, \tag{9}$$

$$\Delta E_p(L) \simeq \frac{2\pi}{L\zeta}x_p, \quad \Delta k_p(L) \simeq \frac{2\pi}{L}s_p. \tag{10}$$

Here, $E_g(L)$, $\Delta E_p(L)$ $[=E_p(L)-E_g(L)]$, and $\Delta k_p(L)$ correspond to the ground-state energy, an excitation gap, and a momentum, respectively. f is free energy per site. Furthermore, the following formulas are available for the Gaussian system:

$$x_p = \frac{1}{2}\left(Kn^2 + \frac{m^2}{K}\right) + (N+\bar{N}), \tag{11}$$

$$s_p = nm + (N-\bar{N}), \tag{12}$$

where (n,m) are the electric and the magnetic charges [6], and $(N,\bar{N})$ are non-negative integers [31].

In the numerical calculations of the above-mentioned excitation levels, the symmetry properties such as the translation of one lattice spacing (a cyclic permutation among sublattices Λ_i) $\mathcal{T}$, the space inversion $\mathcal{P}$, and the spin reversal $\mathcal{S}$ are quite important. This is because these symmetry operations can be also interpreted in the field language as $\mathcal{T}:\sqrt{2}\phi\mapsto\sqrt{2}\phi+2\pi/3$, $\mathcal{P}:\sqrt{2}\phi\mapsto-\sqrt{2}\phi$, and $\mathcal{S}:\sqrt{2}\phi\mapsto\sqrt{2}\phi+\pi$ [7,9,28]. Therefore, the corresponding levels to marginal operators O_0 and O_1 (O_2 and O_3) can be found in the subspace of the wave number $k=0$ and the even parity for both $\mathcal{P}$ and $\mathcal{S}$. On the other hand, the uniform magnetization $s=\sqrt{2}\cos 3\sqrt{2}\phi$ is $k=0$ for $\mathcal{T}$ and even for $\mathcal{P}$, but it is odd for

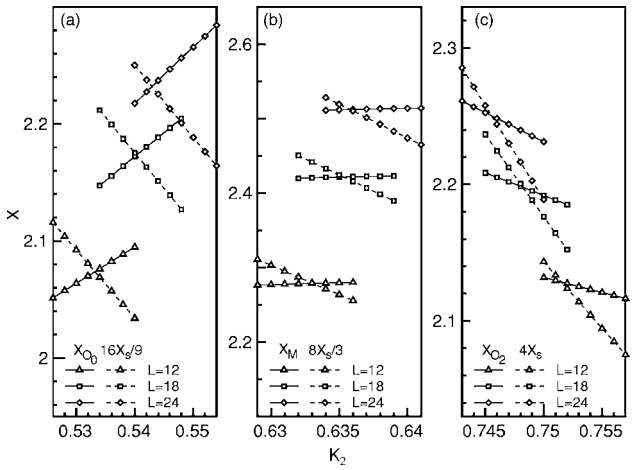

FIG. 2. The K_2 dependence of the scaled gaps at $K_1=1$ (the correspondences between marks and system sizes are given in these panels). (a) [(c)] shows X_{O_0} and $16X_s/9$ (X_{O_2} and $4X_s$). Crossing points give finite-size estimates $v_{\mathrm{U,L}}(u,L)$. (b) gives data $X_{\mathcal{M}}$ and $8X_s/3$ whose crossing points estimate the self-dual line $v_{\mathrm{sd}}(u,L)$.

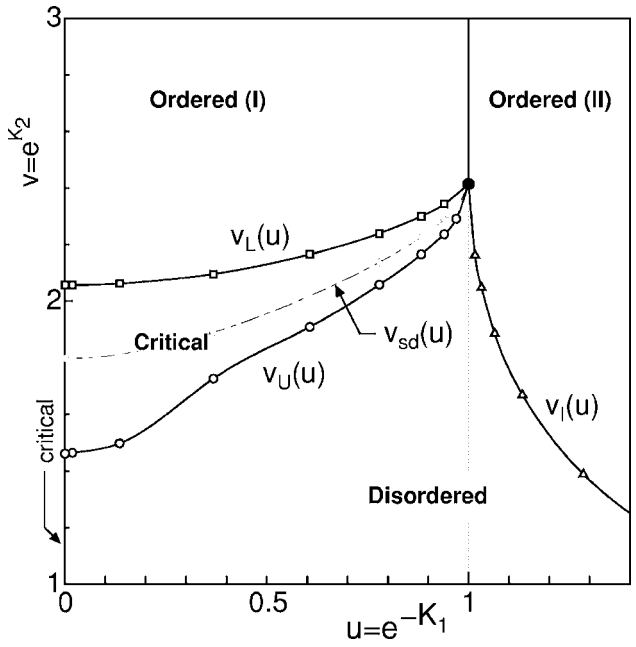

FIG. 3. The phase diagram. Open circles, squares and triangles with curves exhibit the BKT-transition lines $v_{\mathrm{U}}(u)$, $v_{\mathrm{L}}(u)$, and the second-order transition line $v_{\mathrm{I}}(u)$, respectively. The thick vertical line gives the first-order transition boundary. The filled circle at $(1,1+\sqrt{2})$ denotes the decoupling point with the three independent Ising criticality. Diamonds with the dash-dotted line shows $v_{\mathrm{sd}}(u)$.

$\mathcal{S}$ as expected. We thus calculate the excitation levels $\Delta E_p(L)$ by utilizing these symmetry operations and solve the level-crossing conditions (6) and (8), numerically.

Here, the following should be remarked on. When using the KT criterion to determine the BKT-transition points [e.g., $K=\frac{1}{4}$ for $v_{\mathrm{U}}(u)$], we should estimate the Gaussian coupling from an appropriate excitation gap through the former of Eq. (10). If, like the present case, ζ is not known *a priori*, this requires its estimate in advance of the gap data. On the other hand, since the level-crossing conditions (6) and (8) are homogeneous expressions in terms of the scaling dimensions, the corresponding excitation gaps (or scaled ones), instead of the scaling dimensions, can be used to estimate the BKT-transition points. This property is one of the advantages of the level-spectroscopy approach in the studies of 1D quantum and anisotropic 2D classical systems.

III. RESULTS

A. Phase boundaries and the self-dual line

Now we perform the exact-diagonalization calculations of $\mathbf{T}(L)$ for systems up to $L=24$ by the use of the Lanczos algorithm. In Figs. 2(a) and 2(c), we plot examples of the K_2 dependencies of the scaled gaps $X_p(L):=\Delta E_p(L)/(2\pi/L)$ (or values multiplied by constants for convenience) at $K_1=1$. Then, we can find the points at which the above condition (6) or (8) is satisfied [i.e., $v_{\mathrm{U,L}}(u,L)$]. In addition to the logarithmic corrections, there is another type of correction stemming from the $x=4$ irrelevant operators [32], we shall thus extrapolate them to the thermodynamic limit according to the least-squares fitting of the polynomial in $1/L^2$.

In Fig. 3, we give our phase diagram in the 2D model parameter space $(u,v)=(e^{-K_1},e^{K_2})$. The open circles and squares with the solid curves exhibit the lines $v_{\mathrm{U}}(u)$ and $v_{\mathrm{L}}(u)$, respectively, and they separate an intermediate region from the disordered phase and from the ordered phase "Ordered (I)" with sixfold degeneracy. The filled circle at $(u,v)=(1,1+\sqrt{2})$ denotes the decoupling point with three independent Ising criticality. To complete the phase diagram, we also calculate the second-order phase transition point $v_{\mathrm{I}}(u)$ with the Ising criticality in the F region $u>1$, where the finite-size estimates by the PRG method are extrapolated to the thermodynamic limit according to $v_{\mathrm{I}}(u,L)\simeq v_{\mathrm{I}}(u)+a/L^3$ (see the triangles with the solid curve) [33,34]. The ordered phase "Ordered (II)" has the twofold degeneracy, and the thick vertical line shows the first-order phase transition boundary between ordered phases.

For a later discussion, here we mention the self-dual line $v_{\mathrm{sd}}(u)$ embedded in the critical region [35]. Although it is not the phase transition lines, it is expected to be good for numerical calculations [13]. Defining the transformation $6\phi\leftrightarrow\theta$, then we can find the duality relation of the effective model (4), i.e., $(K,y_\phi,y_\theta)\leftrightarrow(1/36K,y_\theta,y_\phi)$. Thus it becomes invariant at $K=\frac{1}{6}$ and $y_\phi=y_\theta$. Since the self-duality provides the degeneracy of excitation levels, e.g., $\cos 6\sqrt{2}\phi$ and $\cos\sqrt{2}\theta$, their crossing provides the finite-size estimates $v_{\mathrm{sd}}(u,L)$. However, these are higher energy excitation levels, and their stable estimations by the Lanczos method are rather difficult. Alternatively, we employ the condition $x_{\mathcal{M}}(l)=8x_s(l)/3$ [$x_{\mathcal{M}}(=2)$ is the dimension of $\mathcal{M}$]; Fig. 2(b) exemplifies the level crossing. Extrapolating them to the thermodynamic limit as $v_{\mathrm{sd}}(u,L)\simeq v_{\mathrm{sd}}(u)+a/L^2$, we determine $v_{\mathrm{sd}}(u)$ (diamonds with the dash-dotted line in Fig. 3), which is between two boundaries $v_{\mathrm{U,L}}(u)$, and is terminated at the critical decoupling point.

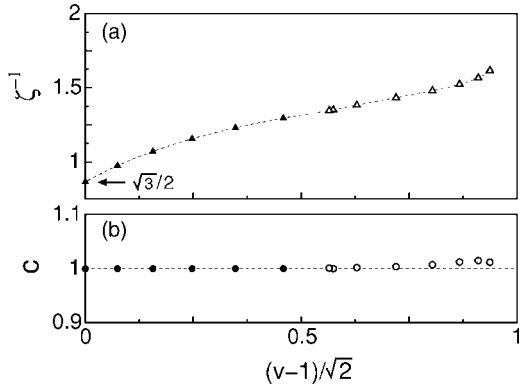

FIG. 4. The inverse effective geometric factor ζ^{-1} (the central charge c) versus $(v-1)/\sqrt{2}$ is plotted in the upper panel (a) [the lower panel (b)]. Filled marks plot the data with $u=0$, and open ones along $v_{sd}(u)$. ζ^{-1} takes the close value to $\sqrt{3}/2$ at $v=1$.

B. Effective geometric factor, central charge, and consistency checks

Although our calculations so far do not need the numerical estimation of ζ, it is necessary to check the criticality and the universal relations among scaling dimensions. For this, following the recent development in the study of 1D quantum systems [36], we focus our attention to the level-1 descendant in the conformal tower of the identity operator, i.e., $\hat{L}_{-1}\mathbf{1}$ in the CFT language. Since the corresponding excitation level is specified by $(n,m,N,\bar{N})=(0,0,1,0)$, we can estimate ζ as

$$\zeta^{-1} = \lim_{L\to\infty} \frac{\Delta E_{\hat{L}_{-1}\mathbf{1}}(L,k=2\pi/L)}{2\pi/L}. \tag{13}$$

The finite-size estimates, i.e., the right-hand side ratio, are extrapolated to the thermodynamic limit by the least-squares fitting of the polynomial in $1/L^2$. Then, we obtain the results which are plotted in Fig. 4(a) (the upper panel). Filled triangles plot the data along the $u=0$ line, and open ones along $v_{sd}(u)$. Here note that since Eq. (13) is only valid for the system with the Gaussian criticality, it does not hold for others including the critical decoupling point. For the isotropic case $v=1$, the estimation excellently agrees with the exact value, and it increases with v as expected. On the other hand, for three decoupled square lattices formed by the anisotropic NNN coupling, ζ^{-1} may equal to $\frac{3}{2}$, so that ζ seemingly jumps at the critical decoupling point. This might have relevance with the jump of the central charge, but a more detailed analysis is left for future study.

Now, according to Eq. (9), we can estimate the central charge c from the L dependence of the ground-state energy $E_g(L)$; the results are plotted in Fig. 4(b) (the lower panel). Although ζ^{-1} increases to nearly twice as large as the isotropic value, the central charge keeps $c=1$ within 1.5% deviations, which clearly demonstrates the Gaussian criticality of the model.

Next, we shall check some relations. Since the amplitudes of the logarithmic corrections are given by the operator-product-expansion coefficients, some universal relations among the scaling dimensions have been discovered: For instance [25,37],

$$\tfrac{1}{3}[2x_0(l)+x_1(l)] \simeq 2 \quad \text{on } v_U(u), \tag{14}$$

$$\tfrac{1}{4}[3x_s(l)+x_4(l)] \simeq \tfrac{1}{2} \quad \text{on } v_L(u). \tag{15}$$

Here, $x_4(l)$ is the scaling dimension of $\sqrt{2}\sin 3\sqrt{2}\phi$, which is $k=0$ for $\mathcal{T}$ and odd for $\mathcal{P}$ and $\mathcal{S}$. In Table I, we give, as an example, the dimensions at $K_1=1$ estimated using the former of Eq. (10). Although $x_0(l)$ and $x_1(l)$ [$x_s(l)$ and $x_4(l)$] largely deviate from the free-boson value 2 $(\frac{1}{2})$ due to the logarithmic corrections, their main parts cancel each other in Eqs. (14) and (15). Therefore, the average x_{av} (x'_{av}), the left-hand side of Eq. (14) [Eq. (15)], takes the value close to 2 $(\frac{1}{2})$. These checks can be passed only if the systems are on the BKT-transition lines $v_{U,L}(u)$, and the numerically utilized levels have the theoretically expected interpretations. Therefore, these are helpful to demonstrate the reliability of our numerical results.

C. Summary of results

Consequently, we can confirm that the intermediate phase shows the Gaussian criticality with $c=1$ which is separated from the sixfold-degenerate ordered and the disordered phases by two BKT-transition lines. Since these are found not to merge into a single curve, the intermediate region as well as the self-dual line continues up to the critical decoupling point, and thus it can be regarded as a realization of the crossover phenomenon from the criticality $c=\frac{3}{2}$ at the point (we shall discuss this issue in Sec. IV) [38]. In the previous researches, one expected that the critical region was terminated at a certain point, and a first-order phase transition between the ordered and disordered phases occurred near the

TABLE I. Examples of the L dependences of the scaling dimensions x_1 and x_4 and the averages x_{av} and x'_{av} (see the text) on the BKT-transition points $v_{U,L}(u)$ $(K_1=1)$. We extrapolate the finite-size estimates to $L\to\infty$ using the least-squares fitting of the polynomial in $1/L^2$.

L	12	15	18	21	24	∞
$x_1(l)$	2.48863	2.50955	2.51917	2.52263	2.52333	
$x_{av}(l)$	1.87339	1.90402	1.92525	1.94038	1.95161	1.988
$x_4(l)$	0.83533	0.80457	0.78318	0.76714	0.75449	
$x'_{av}(l)$	0.49797	0.49447	0.49202	0.49014	0.48862	0.484

critical decoupling point [21,23,39]. But, this possibility is removed. Instead, it is clarified that whereas the obtained phase diagram is, of course, quantitatively different from that in the isotropic case, its structure, the stabilized phases, and the mechanisms of phase transitions are identical to those of the isotropic model [7,24]. Therefore, we conclude that the present model belongs to the 6SC universality class, independently of the spatial anisotropy, and thus KO's assertion is confirmed.

IV. DISCUSSIONS

First, we discuss the nature of our phase diagram (in the isotropic case Qian and Blöte performed the similar analysis [24]). The critical decoupling point with $c=\frac{3}{2}$ becomes unstable against relevant competing perturbations and exhibits crossovers to the behaviors controlled by the critical fixed points with lower symmetries [38]. While one of those perturbations is the energy-density operator of the Ising model with the dimension 1, another one may be a product of the magnetization operators on two of three sublattices which has the dimension $2\times\frac{1}{8}$ [40]. Therefore, the crossover exponent $\phi=(2-\frac{1}{4})/(2-1)=\frac{7}{4}=1.75$ can predict the shape of the boundary around the point. In Fig. 5 the log-log plot of the phase boundary line $v_1(u)$ is given by the triangles with the least-squares-fitting line to the data for the four smallest $|K_1|$ [we define $K_2^*=\ln(1+\sqrt{2})$]. The inverse of the slope estimates the exponent $\phi_F\simeq 1.72$. We also analyze $v_{sd}(u)$, i.e., the crossover line to the Gaussian fixed point with $K=\frac{1}{6}$ (see the diamonds with the fitting line in the same figure). Then, the estimated exponent also takes the close value, i.e., $\phi_{AF}\simeq 1.76$. Therefore, we can confirm the above crossover argument. On the other hand, the analysis of the BKT-transition lines $v_{U,L}(u)$ becomes problematic. This may be mainly due to the existence of the corrections stemming from the marginal operators, while those are absent in the F case.

Second, based on our results obtained in the above, we shall provide some comments on previous work: Miyashita, Kitatani, and Kanada performed the MC simulations at $K_2/K_1=0.2$ and 0.5 [21]. While they used some methods to estimate the transition points, the most specific ones are those by the MC-RG method [41]. They employed the real-space renormalization for each elementary triangle with corner spins s_1, s_2, s_3, i.e., $s_1+s_2+s_3-s_1s_2s_3\mapsto s'$ [42], and then evaluated two BKT-transition points. The comparison between Fig. 3 and their MC-RG data exhibits that the lower-temperature transition point at $K_2/K_1=0.5$ deviates from our phase boundary. One may attribute the discrepancy to the statistical errors in MC simulations, but there might be a possibility that the anisotropy effect could increase an uncontrollability of the real-space RG treatment.

Pajerský and Šurda employed the cluster TM method (a combination of the TM and a mean-field approximation), and claimed that the intermediate critical phase possessed an incommensurate structure [22]. They also implied that the lower-temperature transition between an incommensurate liquid and the commensurate ordered phase was the

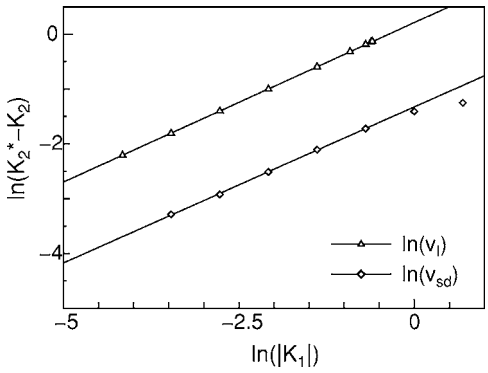

FIG. 5. Log-log plots of the phase boundary line $v_1(u)$ and the self-dual line $v_{sd}(u)$ around the critical decoupling point [we define $K_2^*=\ln(1+\sqrt{2})$]. The least-squares-fitting solid line for triangles (diamonds) estimates the crossover exponent $\phi_F\simeq 1.72$ ($\phi_{AF}\simeq 1.76$) in the F (AF) case.

Pokrovsky-Tarapov type [43]. However, as exhibited, the dual sine-Gordon field theory (4) well describes the phase transitions observed in this model, and there exists no relevant term to stabilize the incommensurate phase [44]. Further, since the duality relation is possessed by the effective model ($u\neq 0$) and it interchanges the transition points in upper and lower temperatures, they should be the same type. Therefore, their observations may be due to an artifact in their mean-field approximation treatment.

de Queiroz and Dommany investigated the same model by the TM calculations [23]. They provided limited evidence for the existence of the BKT phase, and also alternative scenarios including an absence of the BKT phase. Meanwhile, based on the PRG calculation data and the scaled gaps, they drew the qualitative phase diagram including the multicritical point and the direct transition line between ordered and disordered phases. However, it has been pointed out by several authors that the PRG calculations fail to estimate the BKT-transition points [45]; their results suffer from an inadequacy of the method. Further, they tried to check the KT criterion on their phase boundaries. They indeed estimated the exponent η ($=2x_S$) by the use of Eq. (10) and the fixed value $\zeta=2/\sqrt{3}$. But, as we have seen, ζ depends upon model parameters, so the scaled gaps cannot give their universal amplitude in the anisotropic case. Furthermore, their observation that the ratio of scaled gaps gives the flattening region of the parameter is understandable from our viewpoint that approximate cancellation of the geometric factor occurs by taking their ratio. Consequently, these exhibit that the nonuniversal quantity ζ is important in the quantitative description using the numerical calculations, although it is not theoretically important.

To summarize, we investigated the Kitatani-Oguchi model by the level-spectroscopy method in order to clarify spatial anisotropy effects and the global phase diagram. By taking into account the parameter dependence of the geometric factor properly, we analyzed the scaling dimensions of operators around the BKT-transition lines. Then, we numerically determined the phase diagram, where two types of Berezinskii-Kosterlitz-Thouless transition lines separate the intermediate critical phase from the ordered and disordered phases.

Further, we evaluated the central charge and performed consistency checks among scaling dimensions in order to provide evidence of the universality class, and then we confirmed the assertion made by Kitatani and Oguchi. Some comments and comparisons with previous work were also given on the basis of our viewpoint and numerical results.

While our approach has its basis on the argument of the Tomonaga-Luttinger liquid observed in the 1D quantum systems, it is widely applicable to the 2D classical systems with spatial anisotropy.

ACKNOWLEDGMENTS

One of the authors (H.O.) thanks H. Matsuo, M. Nakamura, K. Okunishi, M. Fujimoto, and T. Yokoo for stimulating discussions. We also appreciate H. Kitatani for reading our manuscript prior to submission. Main computations were performed using the facilities of Information Synergy Center, Tohoku University. This work was supported by Grants-in-Aid from the Japan Society for the Promotion of Science.

[1] G. H. Wannier, Phys. Rev. **79**, 357 (1950); Phys. Rev. B **7**, 5017 (1973).
[2] R. M. F. Houtappel, Physica (Amsterdam) **16**, 425 (1950).
[3] K. Husimi and I. Syozi, Prog. Theor. Phys. **5**, 177 (1950); *ibid.* **5**, 341 (1950).
[4] J. Stephenson, J. Math. Phys. **11**, 413 (1970).
[5] H. W. J. Blöte and H. J. Hilhorst, J. Phys. A **15**, L631 (1982).
[6] L. P. Kadanoff, J. Phys. A **11**, 1399 (1978).
[7] B. Nienhuis, H. J. Hilhorst, and H. W. J. Blöte, J. Phys. A **17**, 3559 (1984).
[8] H. W. J. Blöte, M. P. Nightingale, X. N. Wu, and A. Hoogland, Phys. Rev. B **43**, 8751 (1991).
[9] H. W. J. Blöte and M. P. Nightingale, Phys. Rev. B **47**, 15046 (1993).
[10] H. Otsuka and Y. Okabe, Phys. Rev. Lett. **93**, 120601 (2004); Y. Okabe and H. Otsuka J. Phys. A **39**, 9093 (2006).
[11] H. Otsuka, K. Mori, Y. Okabe, and K. Nomura, Phys. Rev. E **72**, 046103 (2005).
[12] H. Otsuka, Y. Okabe, and K. Okunishi, Phys. Rev. E **73**, 035105(R) (2006).
[13] H. Matsuo and K. Nomura, J. Phys. A **39**, 2953 (2006).
[14] H. Kitatani and T. Oguchi, J. Phys. Soc. Jpn. **57**, 1344 (1988).
[15] J. D. Noh and D. Kim, Phys. Rev. E **49**, 1943 (1994); *ibid.* **51**, 226 (1995).
[16] J. Villain and P. Bak, J. Phys. (Paris) **42**, 657 (1981).
[17] D. Kim and P. A. Pearce, J. Phys. A **20**, L451 (1987).
[18] V. L. Berezinskii, Zh. Eksp. Teor. Fiz. **61**, 1144 (1971) [Sov. Phys. JETP **34**, 610 (1972)]; J. M. Kosterlitz and D. J. Thouless, J. Phys. C **6**, 1181 (1973); J. M. Kosterlitz, *ibid.* **7**, 1046 (1974).
[19] J. V. José, L. P. Kadanoff, S. Kirkpatrick, and D. R. Nelson, Phys. Rev. B **16**, 1217 (1977).
[20] H. H. Roomany and H. W. Wyld, Phys. Rev. D **21**, 3341 (1980).
[21] S. Miyashita, H. Kitatani, and Y. Kanada, J. Phys. Soc. Jpn. **60**, 1523 (1991).
[22] P. Pajerský and A. Šurda, J. Stat. Phys. **76**, 1467 (1994).
[23] S. L. A. de Queiroz and E. Domany, Phys. Rev. E **52**, 4768 (1995).
[24] X. Qian and H. W. J. Blöte, Phys. Rev. E **70**, 036112 (2004).
[25] K. Nomura, J. Phys. A **28**, 5451 (1995).
[26] S. Tomonaga, Prog. Theor. Phys. **5**, 544 (1950); J. M. Luttinger, J. Math. Phys. **4**, 1154 (1963); F. D. M. Haldane, J. Phys. C **14**, 2585 (1981).
[27] P. B. Wiegmann, J. Phys. C **11**, 1583 (1978).
[28] D. P. Landau, Phys. Rev. B **27**, 5604 (1983).
[29] J. L. Cardy, J. Phys. A **17**, L385 (1984).
[30] H. W. J. Blöte, J. L. Cardy, and M. P. Nightingale, Phys. Rev. Lett. **56**, 742 (1986); I. Affleck, *ibid.* **56**, 746 (1986).
[31] For example, see P. Ginsparg, in *Fields, Strings and Critical Phenomena*, Proceedings of the Les Houches Summer School, Session XLIX, edited by E. Brézin and J. Zinn Justin (North-Holland, Amsterdam, 1990).
[32] J. L. Cardy, Nucl. Phys. B **270**[FS16], 186 (1986).
[33] M. P. Nightingale, Physica A **83A**, 561 (1976).
[34] B. Derrida and L. De. Seze, J. Phys. (France) **43**, 475 (1982).
[35] For example, P. Lecheminant, A. O. Gogolin, and A. A. Nersesyan, Nucl. Phys. B **639**, 502 (2002).
[36] For example, A. Kitazawa and K. Nomura, J. Phys. Soc. Jpn. **66**, 3944 (1997); M. Nakamura, K. Nomura, and A. Kitazawa, Phys. Rev. Lett. **79**, 3214 (1997).
[37] T. Ziman and H. J. Schulz, Phys. Rev. Lett. **59**, 140 (1987).
[38] A. B. Zamolodchikov, Pis'ma Zh. Eksp. Teor. Fiz. **43**, 565 (1986) [JETP Lett. **43**, 730 (1986)].
[39] M. Mekata, J. Phys. Soc. Jpn. **42**, 76 (1977).
[40] J. M. J. van Leeuven, Phys. Rev. Lett. **34**, 1056 (1975).
[41] M. Kikuchi and Y. Okabe, Prog. Theor. Phys. **78**, 540 (1987).
[42] Th. Niemeijer and J. M. J. van Leeuven, Phys. Rev. Lett. **31**, 1411 (1973).
[43] V. L. Pokrovsky and A. L. Talapov, Phys. Rev. Lett. **42**, 65 (1979); H. J. Schulz, Phys. Rev. B **22**, 5274 (1980).
[44] For the bosonization of the 2D ANNNI model possessing the incommensurate liquid phase, see D. Allen, P. Azaria and P. Lecheminant, J. Phys. A **34**, L305 (2001).
[45] J. C. Bonner and G. Müller, Phys. Rev. B **29**, 5216 (1984); J. Sólyom and T. A. L. Ziman, *ibid.* **30**, 3980 (1984); H. Inoue and K. Nomura, Phys. Lett. A **262**, 96 (1999).